IEEE Access
Multidisciplinary ⋮ Rapid Review ⋮ Open Access Journal

Received January 13, 2021, accepted February 2, 2021, date of publication February 8, 2021, date of current version February 16, 2021.

Digital Object Identifier 10.1109/ACCESS.2021.3057623

Three-Dimensional Generalized Discrete Fuzzy Number and Applications in Color Mathematical Morphology

ZENGTAI GONG, NA QIN, AND GUICANG ZHANG
College of Mathematics and Statistics, Northwest Normal University, Lanzhou 730070, China
Corresponding authors: Na Qin (super_qn@126.com) and Zengtai Gong (zt-gong@163.com)

This work was supported by the National Natural Science Foundation of China under Grant 61763044 and Grant 61861040.

ABSTRACT In this paper, the definition of three-dimensional generalized discrete fuzzy number (3-GDFN) is introduced based on the representation theorem of one-dimensional discrete fuzzy number and the similarity measure definition of two 3-GDFNs is given. Then the concept above mentioned is applied to color image representation and color mathematical morphology (CMM) in RGB space. The basic morphology operators, erosion and dilation, are extended to the CMM by defining the total preorder relation based on similarity measure between two 3-GDFNs instead of general vector sorting methods. The corresponding structuring elements in CMM are variable. Finally, the effectiveness and potential of the theoretical results are verified by comparative experiments. The proposed CMM operators are efficiently used in color image processing.

INDEX TERMS Color mathematical morphology, generalized discrete fuzzy numbers, RGB color space, similarity degree, three-dimensional fuzzy numbers.

I. INTRODUCTION

The concept of fuzzy numbers can be traced back to 1972, Chang and Zadeh [1] called a fuzzy set with special properties on the real number field $\mathbb{R}$ a fuzzy number. Then Voxman [2] proposed the concept of discrete fuzzy numbers which can be used to represent the pixel value in the center point of a window in 2001. In 2004, Wang, Wu, and Zhao gave a representation theorem of discrete fuzzy numbers using r-level sets in [3].

A. APPLICATIONS OF DISCRETE FUZZY NUMBERS

There are many applications of discrete fuzzy numbers in our daily lives, such as image processing, subjective evaluation, decision making, risk analysis, etc. In 2011, Casasnovas and Riera [4] studied the extension of discrete t-norm and t-conorms to discrete fuzzy numbers, they proposed an application to get a group consensus opinion based on discrete fuzzy weighted normed operators. In 2012, Riera and Torrens [5] introduced the aggregation of subjective evaluations based on discrete fuzzy numbers whose support was a subset of consecutive natural numbers belonging to a finite chain L. Then Riera and Torrens [6] presented a linguistic decision-making method based on a couple of discrete aggregation functions which defined on the discrete fuzzy numbers whose support is a set of consecutive natural numbers in 2014. In [7], a new linguistic computational method based on discrete fuzzy numbers was proposed by Massanet *et al.*, ensuring the accuracy and consistency of the application of a multi-expert decision-making problem. Riera *et al.* [8] proposed a fuzzy decision-making model and introduced some interesting properties of the fuzzy linguistic model based on discrete fuzzy numbers. In this linguistic computational model, the experts can use different language levels to evaluate the alternatives more flexibly. In 2015, Riera and Torrens [9] used discrete fuzzy numbers to model complete and incomplete qualitative information and proposed some methods to aggregate such information. The proposed methods were used in a multi-expert decision making problem. In 2015, the definition of generalized discrete fuzzy numbers and the corresponding representation theorem were introduced in [10]. Some weak orders on the one-dimensional generalized discrete fuzzy number space were introduced based on the definition of new addition and multiplication operation. Then Wang *et al.* [11] presented the definition of two-dimensional discrete fuzzy numbers. They set up the weak orders in the two-dimensional

The associate editor coordinating the review of this manuscript and approving it for publication was Emanuele Crisostomi.

This work is licensed under a Creative Commons Attribution 4.0 License. For more information, see https://creativecommons.org/licenses/by/4.0/

discrete fuzzy number space based on the concepts of mass center and ambiguity degree of fuzzy numbers. Then these weak orders were applied to the evaluation of urban natural environment. Zhao *et al.* [12] introduced a novel ranking method based on shape similarity, which was applied to group decision-making problems. This method used symbolic representation to describe each expert's subjective linguistic preference evaluation based on discrete fuzzy numbers.

The above research has made great contributions to the application of discrete fuzzy numbers. However, they still have the following problems from a broader perspective:

1) Most of the current research focuses on the normal discrete fuzzy numbers, which must include the elements with a membership function value of 1. But in applications, the non-normal discrete fuzzy numbers are often used [10].
2) In addition, the one-dimensional discrete fuzzy number can be only represented and processed single channel digital signal, but it is not suitable for vague multichannel digital information processing. For example, one-dimensional discrete fuzzy numbers cannot be used for color images because the pixel values in RGB color space can be composed of three basic colors: red, green and blue. In this case, the pixel values of a color image can only be represented by means of three-dimensional discrete fuzzy numbers.
3) There are few researches on the application of discrete fuzzy numbers to the representation and processing of color images.
4) Fuzzy numbers need to be sorted in many application problems, but there is no universally accepted standard for the definition of the order relation between discrete fuzzy numbers.

Therefore, we extend the discrete fuzzy numbers to three-dimensional generalized discrete fuzzy numbers(3-GDFN). On one hand, the non-normal discrete fuzzy number has a wider range of application, and the normal discrete fuzzy number is a special case of the generalized discrete fuzzy number (Remark 2). On the other hand, the three-dimensional discrete fuzzy number can be used to deal with multi-channel digital information and multi-criteria evaluation problem (Example 5.1 and Example 5.2 in [11]). In this paper, we further define the order relationship based on fuzzy similarity in 3-GDFN space and explore its application in color image processing.

B. COLOR MATHEMATICAL MORPHOLOGY

Mathematical morphology is widely used in image processing and analysis, which includes the image filtering, image denoising, edge detection, texture analysis, shape analysis or image segmentation. It is a simple and efficient nonlinear processing technology, which consists of basic dilation operator and erosion operator. Mathematical morphology is first introduced in binary images processing by Matheron and Serra [13]–[15]. Due to its strict mathematical foundation and ability to deal with the spatial relationship of image pixels, it is extended to gray-scale images processing [16]. The research object of gray-scale morphology is the digital image function. Since the gray image is a scalar function, the maximum and minimum operations are used instead of the set operations of binary morphology to define gray-scale morphological operators [16].

Fuzzy set theory can also be used to extend binary morphology to gray-scale morphology, since ambiguity is an intrinsic property of digital images. The idea of De Baets [17] was to fuzzify the basic logical operations, the intersection and inclusion in binary morphology are replaced by fuzzy conjunction and fuzzy implication. Bloch and Maître [18] used a similar method to De Baets. The difference is that they use a t-norm to define fuzzy dilation instead of conjunction, and then use the associated residual implication to define fuzzy erosion. M. Nachtegael and E.E. Kerre [19] presented a general logical framework for fuzzy mathematical morphology and researched the connections between binary, gray-scale and fuzzy mathematical morphologies in [20]. Furthermore, Mélange et.al. [21] constructed the interval-valued fuzzy morphological operators. Sussner et.al. [22] researched the interval-valued and intuitionistic fuzzy mathematical morphologies.

The color mathematical morphology (CMM) is the theory of extending the binary or gray-scale mathematical morphology to color image space. However, there are many challenges because of the vector nature of color pixels. In many literatures, the definition of different color sorting methods is the basis of CMM operation [23]. Barnett [24] proposed four types of vector sorting methods: marginal (M), conditional (C), partial (P) and reduced (R) sorting approaches. These sorting approaches have certain drawbacks when they are used for CMM according to different application environments. For instance, the M-ordering [25] is the pointwise ordering method of the color components, which will produce false colors in original image. The C-ordering, also known as lexicographic ordering [26], will generate visual nonlinear effects from the perspective of human visual perception. Because some component has priority over others when vectors are sorted. The P-ordering [27] and R-ordering [28] rely on manually specified pre-sorting operations, which lack antisymmetry property and also have the problem of visual perceptual nonlinearities [29], [30].

In order to solve the above problems, many sorting-based CMM algorithms are proposed. A novel vector sorting method for color image morphological processing based on fuzzy sets, umbra and threshold techniques was proposed in [31]. The color vectors were sorted by their distance to the black and white pixels respectively. Bouchet *et al.* [32] used a fuzzy order based on fuzzy preference relation to create a total order complete lattice in RGB color space. The three fuzzy preference relations were then aggregated with the arithmetic mean. Experimental results showed that the proposed color morphological operators can be efficiently used for color image processing. A conditionally invariant

mathematical morphological framework for color images was presented in [33], and a vector ordering method based on linear transformations from RGB to other color spaces and principal component analysis (PCA) were developed. Valle and Valente [34] proposed a quantal-based approach to color mathematical morphology based on the CIEL*a*b* color space in spherical coordinates. The definition of morphological operators used a distance-based ordering scheme and non-flat structuring elements. These operators achieved good results in color image edge extraction experiments. Pedro Bibiloni et.al. [35] generalized fuzzy mathematical morphology to process multivariate images in the CIEL*a*b* color space and introduced soft color erosion and soft color dilation operators. Several visual examples were presented to provide insights into this approach. These visual examples included different morphological operators applied to natural and artificial images. A fuzzy mathematical morphology based on Intuitionistic fuzzy sets to leukocytes segmentation was presented in [36]. The main idea was to model color images as an Intuitionistic fuzzy set based on hue components in the HSV color space. Then, a pixel labeled as leukocyte was selected and compared to the entire image through a similarity measure. Experimental results showed that the classification accuracy and precision were higher. Al-Otum [37] presented a new set of color image morphological operators based on an improved vector distance measure. The color pixels were divided into different categories in the HSV color model, then the color distance metric was calculated according to the category of each input color pixel, and finally the color morphological operator was obtained using the combination technique. The designed operators were applied to edge detection, skeletonisation, noise suppression, texture and shape analysis.

Based on the inspiration of the above literature, we explored the application of three-dimensional generalized discrete fuzzy number theory in the color mathematical morphology. In our method, the three-dimensional generalized discrete fuzzy number is used to express the pixel value of color image in the RGB space. It is because the three components of the RGB model have the same properties. Next, the fuzzy similarity measure between 3-GDFNs is introduced and used to define the total preorder relationship in 3-GDFNs. Finally, we use the order relation based on fuzzy similarity measure to define the basic operators of color mathematical morphology. These basic operators are of great significance to the analysis and processing of color images.

C. GOAL OF THIS WORK

The goal of this paper is to study the basic theory of 3-GDFN and its application in color mathematical morphology. The structuring elements and basic operators of CMM are defined based on the fuzzy similarity measure, and the processing and analysis of color images are achieved through the combination of these operators.

The novelty of this paper can be shown as follows:

1) The definition of 3-GDFN is given based on the representation theorem of one-dimensional discrete fuzzy number and the 3-GDFNs are used to represent the pixel values of color images in RGB space.
2) The color morphological operators (erosion and dilation) are constructed by the order relation based on 3-GDFNs similarity measure.

The remainder of this paper is organized as follows: In section 2, we briefly review the basic definitions and results about fuzzy numbers and generalized discrete fuzzy numbers. In section 3, we give the concept and theorem about 3-GDFNs, and define the fuzzy similarity measure of two 3-GDFNs. In section 4, we construct the three-dimension generalized discrete fuzzy representation of a color image, and establish the basic mathematical morphology operators by the fuzzy similarity. Lots of comparable experiments are presented in section 5. Finally, the conclusions are described in section 6.

II. PRELIMINARIES

In this section, we will introduce basic concepts about generalized discrete fuzzy numbers(GDFN) and their representation theorem.

Let $\mathbb{R}^n$ be the n-dimensional Euclidean space. A fuzzy set of $\mathbb{R}^n$ is a mapping $u : \mathbb{R}^n \to [0, 1]$. For each fuzzy set u of $\mathbb{R}^n$, let $[u]^r = \{x \in \mathbb{R}^n : u(x) \geq r\}$ for any $r \in (0, 1]$ be its r-level set. By supp(u) we denote the support of u, i.e., supp(u)=$\{x \in \mathbb{R}^n : u(x) > 0\}$. In addition, we denote the closure of supp(u) by $[u]^0$, i.e., $[u]^0 = \overline{\{x \in \mathbb{R}^n : u(x) > 0\}}$.

Definition 1 [10]: Let $\omega \in (0, 1]$. A fuzzy set $u : \mathbb{R} \to [0, \omega]$ is called a generalized discrete fuzzy number if its support is finite, i.e., there exist $x_1, x_2, \ldots, x_n \in \mathbb{R}$ with $x_1 < x_2 < \ldots < x_n$ such that $[u]^0 = \{x_1, x_2, \ldots, x_n\}$, and there exist natural numbers s,t with $1 \leq s \leq t \leq n$ such that

(1) $u(x_i) = \omega$ for any natural number i with $s \leq i \leq t$;
(2) $u(x_i) \leq u(x_j)$ for any natural numbers i,j with $1 \leq i \leq j \leq s$;
(3) $u(x_i) \geq u(x_j)$ for any natural numbers i,j with $t \leq i \leq j \leq n$.

We denote the collection of all generalized discrete fuzzy numbers by GDFN.

Remark 2: : In Definition 1, when $\omega = 1$, u is a discrete fuzzy number.

Theorem 3 [10]: Let $\omega \in (0, 1]$ and $u \in$ GDFN with the maximum membership degree ω. Then

(1) $[u]^r$ is a nonempty finite subset of R for any $r \in [0, \omega]$;
(2) $[u]^{r_2} \subseteq [u]^{r_1}$ for any r_1,$r_2 \in [0, \omega]$ with $r_1 \leq r_2$;
(3) $\{x \in [u]^0 : \min[u]^r \leq x \leq \max[u]^r\} \subset [u]^r$ for any $r \in [0, \omega]$;
(4) For any $r_0 \in (0, \omega]$, there exist real number r_0' with $0 < r_0' < r_0$ such that $[u]^{r_0'} = [u]^{r_0}$ (i.e., $[u]^r = [u]^{r_0}$ for any $r \in [r_0', r_0]$).

Conversely, if for any $r \in [0, \omega]$ with $\omega \in (0, 1]$, there exists $A_r \subset \mathbb{R}$ satisfying

(i) A_r is nonempty and finite for any $r \in [0, \omega]$;

(ii) $A_{r_2} \subseteq A_{r_1}$ for any $r_1, r_2 \in [0, \omega]$ with $r_1 \leq r_2$;
(iii) $\{x \in A_0 : \min A_r \leq x \leq \max A_r\} \subset A_r$ for any $r \in [0, \omega]$;
(iv) For any $r_0 \in (0, \omega]$, there exist a real number r_0' with $0 < r_0' < r_0$ such that $A_{r_0'} = A_{r_0}$ (i.e., $A_r = A_{r_0}$ for any $r \in [r_0', r_0]$),

then there exists a unique $u \in$ GDFN with the maximum membership degree ω such that $[u]^r = A_r$ for any $r \in [0, \omega]$.

III. THREE-DIMENSIONAL GENERALIZED DISCRETE FUZZY NUMBER

Let $X = (x_1, x_2, x_3)$, $Y = (y_1, y_2, y_3) \in \mathbb{R}^3$, define $X \leq\leq\leq Y$ or $Y \geq\geq\geq X$, if and only if $x_i \leq y_i, i = 1, 2, 3$. Let us consider the set $A = \{X_1, X_2, \ldots, X_m\}$ with $X_j = (x_{j1}, x_{j2}, x_{j3}) \in \mathbb{R}^3, j = 1, 2, \ldots, m$, we define

$$\begin{aligned} \min A &= \wedge_{j=1}^{m} X_j \\ &= (\min_{1\leq j\leq m}\{x_{j1}\}, \min_{1\leq j\leq m}\{x_{j2}\}, \min_{1\leq j\leq m}\{x_{j3}\}) \quad (1) \\ \max A &= \vee_{j=1}^{m} X_j \\ &= (\max_{1\leq j\leq m}\{x_{j1}\}, \max_{1\leq j\leq m}\{x_{j2}\}, \max_{1\leq j\leq m}\{x_{j3}\}) \quad (2) \end{aligned}$$

It is obvious that $\min A$ and $\max A$ do not necessarily belong to the set of A. Now, we will define three-dimensional generalized discrete fuzzy number using the representation theorem 3.

A. DEFINITION

Definition 4: Let $\omega \in (0, 1]$, a fuzzy set $u : \mathbb{R}^3 \to [0, \omega]$ is called three-dimensional generalized discrete fuzzy number if it satisfies the following four conditions:

(1) $[u]^r$ is a nonempty finite subset of $\mathbb{R}^3$ for any $r \in [0, \omega]$;
(2) $[u]^{r_2} \subseteq [u]^{r_1}$ for any $r_1, r_2 \in [0, \omega]$ with $0 \leq r_1 \leq r_2 \leq \omega$;
(3) For any $r \in [0, \omega]$, $\{X \in [u]^0 : \min[u]^r \leq\leq\leq X \leq\leq\leq \max[u]^r\} \subset [u]^r$;
(4) For any $r_0 \in (0, \omega]$, there exist some real numbers r_0' with $0 < r_0' < r_0$ such that $[u]^{r_0'} = [u]^{r_0}$ (i.e., $[u]^r = [u]^{r_0}$ for any $r \in [r_0', r_0]$).

We denote the collection of all three-dimensional generalized discrete fuzzy numbers by 3-GDFN.

Example 5: Let $\omega = 0.95$, $u : \mathbb{R}^3 \to [0, \omega]$ be defined as follows:

$$u(X) = \begin{cases} 0.95, & X = X_6 \\ 0.72, & X = X_5 \\ 0.65, & X = X_4, X_7 \\ 0.28, & X = X_3, X_8 \\ 0.13, & X = X_1, X_2, X_9 \\ 0, & \text{otherwise.} \end{cases}$$

where, $X_1 = (1, 1, 1), X_2 = (1, 8, 1), X_3 = (2, 3, 2), X_4 = (3, 5, 3), X_5 = (4, 6, 4), X_6 = (5, 5, 5), X_7 = (6, 6, 3), X_8 = (8, 3, 2), X_9 = (8, 7, 1)$. Then u is a three-dimensional generalized discrete fuzzy number with $[u]^0 = \{X_1, X_2, \ldots, X_9\}$.

Theorem 6: Let $\omega \in (0, 1]$, $u_1, u_2, u_3 \in$ GDFN, if $u : \mathbb{R}^3 \to [0, \omega]$ is defined by $u(x, y, z) = \min(u_1(x), u_2(y), u_3(z))$ for any $(x, y, z) \in \mathbb{R}^3$, then $u \in$ 3-GDFN.

Proof: We need to proof that u meets the above four conditions of the Definition 4.

(1) Let $u_1, u_2, u_3 \in$ GDFN, and $u(x, y, z) = \min(u_1(x), u_2(y), u_3(z))$ for $(x, y, z) \in \mathbb{R}^3$, clearly, for any $r \in [0, \omega]$, the support of u is nonempty and finite.
(2) Let $\forall r_1, r_2 \in [0, \omega]$ with $0 \leq r_1 \leq r_2 \leq \omega$, clearly, if $r_1 = r_2$ then u defined above is $[u]^{r_2} = [u]^{r_1}$. Let $\forall x \in [u_1]^{r_2}$, $\forall y \in [u_2]^{r_2}$,$\forall z \in [u_3]^{r_2}$, we know that $u(x, y, z) = \min(u_1(x), u_2(y), u_3(z))$, so $(x, y, z) \in [u]^{r_2}$. And because $u_1, u_2, u_3 \in$ GDFN, it is obvious that $[u_1]^{r_2} \subseteq [u_1]^{r_1}$, $[u_2]^{r_2} \subseteq [u_2]^{r_1}$, $[u_3]^{r_2} \subseteq [u_3]^{r_1}$, so $x \in [u_1]^{r_1}$, $y \in [u_2]^{r_1}$,$z \in [u_3]^{r_1}$, i.e., $(x, y, z) \in [u]^{r_1}$. So,$[u]^{r_2} \subset [u]^{r_1}$. Thus,$[u]^{r_2} \subseteq [u]^{r_1}$ with $0 \leq r_1 \leq r_2 \leq \omega$. The condition (2) holds.
(3) Let $A \triangleq \{X \in [u]^0 : \min[u]^r \leq\leq\leq X \leq\leq\leq \max[u]^r\}$ for any $r \in [0, \omega]$. Suppose that the number of three-dimensional vectors X_j is m in $[u]^r$, where $X_j = (x_{j1}, x_{j2}, x_{j3}), j = 1, 2, \ldots, m$, so we know
$\min[u]^r = \wedge_{j=1}^{m} X_j =$
$\{\min_{1\leq j\leq m}\{x_{j1}\}, \min_{1\leq j\leq m}\{x_{j2}\}, \min_{1\leq j\leq m}\{x_{j3}\}\}$,
$\max[u]^r = \vee_{j=1}^{m} X_j =$
$\{\max_{1\leq j\leq m}\{x_{j1}\}, \max_{1\leq j\leq m}\{x_{j2}\}, \max_{1\leq j\leq m}\{x_{j3}\}\}$.
Let $\forall (a, b, c) \in A$, so we know $(a, b, c) \in [u]^0$ and fulfill $\min_{1\leq j\leq m}\{x_{j1}\} \leq a \leq \max_{1\leq j\leq m}\{x_{j1}\}$, $\min_{1\leq j\leq m}\{x_{j2}\} \leq b \leq \max_{1\leq j\leq m}\{x_{j2}\}$, $\min_{1\leq j\leq m}\{x_{j3}\} \leq c \leq \max_{1\leq j\leq m}\{x_{j3}\}$. Because $u(a, b, c) = \min(u_1(a), u_2(b), u_3(c))$, so $u_1(a) > r, u_2(b) > r, u_3(c) > r$, this means $u(a, b, c) > r$ i.e., $(a, b, c) \in [u]^r$ for any $r \in [0, \omega]$, thus $A \subset [u]^r$. The condition (3) holds.
(4) Suppose that $r_0 \in (0, \omega]$, if $r_0 \leq r_1'$, there exist some real number r_0', such that $0 < r_0' < r_0 \leq r_1'$. So for $\forall r \in [r_0', r_0]$, $[u]^r = [u]^{r_0} = [u]^0$. If $r_0 > r_1'$, there exist a natural number i_0 fulfill $1 < i_0 \leq n_0$, such that $r_{i_0} < r_0 \leq r_{i_0+1}$. So there must exist a real number r_0', such that $r_{i_0} < r_0' < r_0 \leq r_{i_0+1}$, so we know, for $\forall r \in [r_0', r_0]$, $[u]^r = [u]^{r_0} = [u]^{r_{i_0+1}}$. Above that for $\forall r \in [r_0', r_0]$, $[u]^r = [u]^{r_0}$.

Therefore, the proof is complete. □

Because the Theorem 6 allows us to define a type of three-dimensional generalized discrete fuzzy number from a triplet of GDFN. In this way, we propose the following Definition 7.

Definition 7: Let $\omega \in (0, 1]$, $u_1, u_2, u_3 \in$ GDFN with $[u_1]^0 = \{x_1, x_2, \ldots, x_m\}$, $[u_2]^0 = \{y_1, y_2, \ldots, y_m\}$, $[u_3]^0 = \{z_1, z_2, \ldots, z_m\}$. We call the three dimensional generalized discrete fuzzy number $u : \mathbb{R}^3 \to [0, \omega]$ defined by $u(x, y, z) = \min(u_1(x), u_2(y), u_3(z))$, $x \in \{x_1, x_2, \ldots, x_m\}$, $y \in \{y_1, y_2, \ldots, y_m\}$, $z \in \{z_1, z_2, \ldots, z_m\}$, $(x, y, z) \in \mathbb{R}^3$ is three dimensional unite generalized discrete fuzzy number of u_1, u_2 and u_3. And we denote the collection of all three dimensional unite generalized discrete fuzzy number by $\bigcup$(3-GDFN).

Next, we define the mean value of three-dimensional generalized discrete fuzzy number.

Definition 8: Let $u \in$ 3-GDFN, $[u]^0 = \{X_1, X_2, \ldots, X_n\}$, $X_i = (x_{i1}, x_{i2}, x_{i3})$, $i = 1, 2, \ldots, n$.
The mean value of u is defined as follows:

$$\overline{M}(u) = (\overline{x_1}, \overline{x_2}, \overline{x_3}) = \frac{\sum_{i=1}^{n} u(X_i)X_i}{\sum_{i=1}^{n} u(X_i)} \tag{3}$$

B. SIMILARITY BETWEEN 3-GDFNs

We need a similarity measure to compare the closeness of two fuzzy sets. It is generally required that the measures used for comparison must fulfill the following natural attributes: the similarity should be non-negative and symmetric, and the similarity of two identical fuzzy sets should be 1. Therefore, a reasonable definition of similarity must satisfy at least the following conditions.

Definition 9 [38]: For the uniform U, the collection of fuzzy sets on U is $\mathcal{F}(U)$, let $A, B \in \mathcal{F}(U)$, the mapping $\sigma : \mathcal{F}(U) \times \mathcal{F}(U) \to [0, 1]$ is called a similarity measure if it satisfies the following properties:

(1) $\sigma(A, A) = 1$;
(2) $\sigma(\emptyset, U) = 0$;
(3) $\sigma(A, B) = \sigma(B, A)$;
(4) For all $A, B, C \in \mathcal{F}(U), A \subseteq B \subseteq C \Rightarrow \sigma(A, C) \leq \min(\sigma(A, B), \sigma(B, C))$.

So, $\sigma(A, B)$ is the similarity degree between A and B.

This is the axiomatic definition of similarity. Now we need the similarity measures between 3-GDFNs. There are three main types of fuzzy similarity measures [38] methods proposed in many literatures. (1) distance-based measures, (2) set-theoretic based measures and (3) implication-based measures [39]. In this paper, the similarity measures between 3-GDFNs are designed using fuzzy logic operators.

The definition of the similarity measures between two 3-GDFNs is as follows:

Definition 10: Let $u, v \in$ 3-GDFN, $[u]^0 = \{X_1, X_2, \ldots, X_n\}, X_i = (x_{i1}, x_{i2}, x_{i3})$ and $[v]^0 = \{Y_1, Y_2, \ldots, Y_n\}, Y_i = (y_{i1}, y_{i2}, y_{i3})$, $i = 1, 2, \ldots, n$. The similarity between u and v is defined $\sigma(u, v)$ as following:

$$\sigma(u, v) \triangleq \frac{\sum_{i=1}^{n} \min(u(x_{i1}, x_{i2}, x_{i3}), v(y_{i1}, y_{i2}, y_{i3}))}{\sum_{i=1}^{n} \max(u(x_{i1}, x_{i2}, x_{i3}), v(y_{i1}, y_{i2}, y_{i3}))} \tag{4}$$

Based on the above definition, we will introduce the application of 3-GDFN in color image mathematical morphology in the next section.

IV. APPLICATION OF 3-GDFN ON COLOR MATHEMATICS MORPHOLOGY

The color image is modeled as functions $f : D_f \subset \mathbb{R}^2 \to \tau \subset \mathbb{R}^3$, where D_f is the domain of image, τ is the corresponding color space. In this section, we apply the above definition of 3-GDFN in section III to CMM, and formally introduce its structuring elements and basic operators.

A. COLOR IMAGE IN RGB SPACE

There are many different representations of color space [40]. In the processing and analysis of color images, the selection of an appropriate color space representation is still a difficult task [41]. In this paper, a three-dimensional generalized discrete fuzzy number is constructed for each pixel of a color image based on the RGB color model. The RGB model is the most direct representation of color images and is widely used in computer software and hardware systems. It is established in a Cartesian coordinate system. An image in this model is composed by three images, each of them corresponding with a primary color: red(R), green(G) and blue(B), and the three components have the same properties. One possible way to process color images is to process these three components individually. For the above reasons, we will interpret color images in RGB space as 3-GDFN in the next subsection.

B. INTERPRETATION OF COLOR IMAGE AS 3-GDFN

To express a color image with three-dimensional generalized discrete fuzzy numbers, the following steps are required.

- We take a color image I in RGB space for example, the size of I is $M \times N \times 3$. Let $I(x, y)$ represents a three dimensional pixel value of point (x, y) in I, where $x \in \{1, 2, \ldots, M\}$, $y \in \{1, 2, \ldots, N\}$. We denote $I(x, y) = (I_1(x, y), I_2(x, y), I_3(x, y))$, where $I_k(x, y) \in \{0, 1, 2, \ldots, 255\}, k = 1, 2, 3$.
- We take a point $(x_0, y_0), x_0 \in \{2, 3, \ldots, M-1\}, y_0 \in \{2, 3, \ldots, N-1\}$ in I as the center and use the eight neighboring pixels around it to form a cube, denoted as W. The size of W is $3 \times 3 \times 3$. The point in W can be expressed as $(x_0 + i, y_0 + j), i, j = \{-1, 0, 1\}$ and the corresponding pixel value can be expressed as $I_k(x_0 + i, y_0 + j), i, j = \{-1, 0, 1\}, k = 1, 2, 3$.
- In order to represent color pixel values by 3-GDFN, we calculate the mean value $\overline{W} = (\overline{W}_1, \overline{W}_2, \overline{W}_3)$ and standard deviation $\overline{S} = (\overline{S}_1, \overline{S}_2, \overline{S}_3)$ of W.

$$\overline{W}_k = \frac{\sum_{i=-1}^{1} \sum_{j=-1}^{1} I_k(x_0 + i, y_0 + j)}{3 \times 3} \tag{5}$$

where $k = 1, 2, 3$.

$$\overline{S}_k = \sqrt{\frac{\sum_{i=-1}^{1} \sum_{j=-1}^{1} (I_k(x_0 + i, y_0 + j) - \overline{W}_k)^2}{3 \times 3 - 1}} \tag{6}$$

where $k = 1, 2, 3$.

- We construct generalized Gaussian discrete fuzzy numbers for $I_k(x_0, y_0), k = \{1, 2, 3\}$. Let $\omega \in (0, 1]$, we define $u_k : \mathbb{R} \to [0, \omega]$ is

$$u_k(I_k(x, y)) = \begin{cases} \exp(-\frac{(I_k(x,y) - \overline{W}_k)^2}{2\overline{S}_k^2}), & \text{if } (x, y) \in W \\ 0, & \text{otherwise.} \end{cases} \tag{7}$$

where $k = \{1, 2, 3\}$, then $u_1, u_2, u_3 \in$ GDFN with $[u_k]^0 = \{I_k(x_0 + i, y_0 + j) | i, j = \{-1, 0, 1\}\}$.

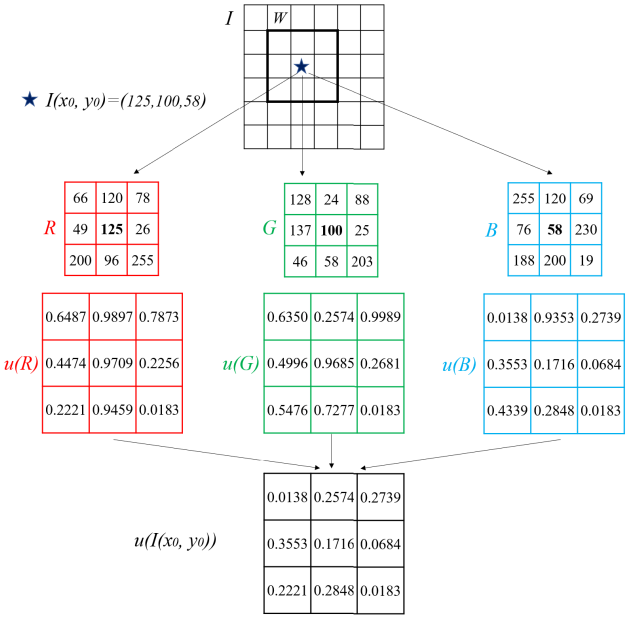

FIGURE 1. Using 3-GDFN to represent pixel value of color images.

- According to Definition 7, we define $u : \mathbb{R}^3 \to [0, \omega], \omega \in (0, 1]$ is that

$$u(I(x, y)) = \min(u_1(I_1(x, y)), u_2(I_2(x, y)), u_3(I_3(x, y))). \tag{8}$$

then u is a three-dimensional generalized discrete fuzzy number that satisfies $[u]^0 = \{I(x_0 + i, y_0 + j)|i, j = \{-1, 0, 1\}\}$.

Example 11: Let I be a color image in RGB space. We use the point (x_0, y_0) as a center and take its eight neighboring pixels to form a cube W. Fig.1 shows the different objects I, $I(x_0, y_0)$ and the decomposition of W in the three components of RGB space. As an example, we give some values of W in each component. When $I(x_0, y_0) = (125, 100, 58)$, its 3-GDFN representation is shown in Fig.1.

We interpret each pixel value of the color image in RGB space as 3-GDFN. The above method can also be applied to other color spaces. Next, we will define the structuring elements and basic operators of the CMM based on the 3-GDFN space. Therefore, the morphological approach in this paper is also applicable to other color spaces.

C. STRUCTURING ELEMENTS

In Mathematical Morphology, the structuring element (SE) is a set used to examine the geometrical structures of an image. The size and shape of the SE are chosen according to the different application environments. In order to compare each element of the SE with the image, the SE is moved in the image so that it covers the entire image pixel by pixel. The SE plays an important role in the definition of CMM. In general, the SE indicates the neighborhood over which the pixels of the image are compared. The general definition of SE is as follows:

Definition 12 [32]: Let $f : D_f \subset \mathbb{R}^2 \to \mathbb{R}^3$ be a color image, let $c \in D_f$ be a pixel point, and let (D_f, d) be a metric space. A structuring element (SE) for the color pixel point c is a neighborhood:

$$B(c, r) = \{\tilde{c} \in D_f : d(c, \tilde{c}) \leq r\} \tag{9}$$

where r denotes any positive real number, which is called diameter.

In classical Mathematical Morphology, the fixed-size structuring elements are used without considering the local features of the image. When an image contains multiple objects with large differences, the corresponding morphological operator can hardly achieve better processing results. Therefore, the adaptive structuring elements that adjust the size and shape according to the local characteristics of the image have become the research direction.

According to the 3-GDFN representation of color pixel value and the definition of fuzzy similarity measure, we construct the structuring elements with variable shape as following steps:

- Let I be a color image in RGB space, and $I(x, y)$ is the pixels value of I. Taking the point $(\tilde{x}, \tilde{y})$ as the center, and the connected pixels around it form an area G with the size of $n \times n$, where $n \geq 3$ and n is odd. When $n = 3$, $G_{3\times3}$ is expressed as follows:

$$G_{3\times3} = \begin{pmatrix} I(\tilde{x}-1, \tilde{y}-1) & I(\tilde{x}, \tilde{y}-1) & I(\tilde{x}+1, \tilde{y}-1) \\ I(\tilde{x}-1, \tilde{y}) & I(\tilde{x}, \tilde{y}) & I(\tilde{x}+1, \tilde{y}) \\ I(\tilde{x}-1, \tilde{y}+1) & I(\tilde{x}, \tilde{y}+1) & I(\tilde{x}+1, \tilde{y}+1) \end{pmatrix}$$

- We construct the 3-GDFN representation for each pixel value in G according to (7) and (8) and denote them as $u^1, u^2, \ldots, u^{n\times n}$ in G'. When $n = 3$, $G'_{3\times3}$ is expressed as follows:

$$G'_{3\times3} = \begin{pmatrix} u^1 & u^2 & u^3 \\ u^4 & u^5 & u^6 \\ u^7 & u^8 & u^9 \end{pmatrix}$$

- According to (4), we calculate the fuzzy similarity between the center 3-GDFN(e.g. u^5 in $G'_{3\times3}$) and the surrounding 3-GDFNs of the area G' respectively.
- Let $\lambda \in [0, 1]$, the structuring element for the point $(\tilde{x}, \tilde{y})$ is a neighborhood:

$$B((\tilde{x}, \tilde{y}), \lambda) = \{(x, y) \in G : \sigma(u(I(x, y)), u(I(\tilde{x}, \tilde{y}))) \geq \lambda\} \tag{10}$$

It is obvious that if the value of λ is 0, the SE is the area G itself. The shape of SE changes according to λ, and can be flexibly adjusted according to different application requirements.

Example 13: When $n = 3$, we assume that the fuzzy similarity is calculated as follows:

	u^1	u^2	u^3	u^4	u^5	u^6	u^7	u^8	u^9
u^5	0.4	0.6	1	0.3	1	0.5	0.2	1	1

If $\lambda = 0.3$, the shape of SE is shown as follows:

$$\begin{pmatrix} \bullet & \bullet & \bullet \\ \bullet & \bullet & \bullet \\ \circ & \bullet & \bullet \end{pmatrix}$$

If $\lambda = 1$, the shape of SE is shown as follows:

$$\begin{pmatrix} \circ & \circ & \bullet \\ \circ & \bullet & \circ \\ \circ & \bullet & \bullet \end{pmatrix}$$

where, symbols $\bullet$ and $\circ$ represent that the corresponding pixel point belongs to or does not belong to the structuring element respectively.

According to the steps shown above, we can take the parameter $\lambda = 0$ and choose G of other shapes and sizes. Therefore, the method in this paper is compatible with the shape and structure analysis function of classical morphological methods.

D. MORPHOLOGICAL OPERATORS FOR COLOR IMAGES

The operators of color mathematical morphology based on 3-GDFN are introduced in this subsection. As mentioned earlier, the definition of basic erosion and dilation operators requires a complete lattice structure in the color image space. This complete lattice depends on the order relationship between the elements in color images.

Definition 14 [15]: Let $\leq_\tau$ be an order on $\tau \subset \mathbb{R}^3$. The space of functions from D_f to τ with the order $\leq$ defined as

$$f \leq g \Leftrightarrow f(x) \leq_\tau g(x), \forall x \in D_f \tag{11}$$

for any $f, g : D_f \subseteq \mathbb{R}^2 \to \tau \subseteq \mathbb{R}^3$ has a lattice structure.

Definition 15 [32]: Let $\tau \subset \mathbb{R}^3$ be a color space with complete lattice structure by a total order $\leq_\tau$. Let B be the structuring element, the basic operators erosion ϵ and dilation δ of the color image f are defined as follows:

$$\epsilon(f) = \inf_{x \in B}\{f \circ T_x\} \tag{12}$$

$$\delta(f) = \sup_{x \in B}\{f \circ T_{-x}\} \tag{13}$$

where $T_x : \mathbb{R}^2 \to \mathbb{R}^2$ is the translation function by the element $x \in \mathbb{R}^2$, that is $T_x(s) = s + x$.

According to the previous definition, in order to perform the erosion or dilation of an input image f by the structuring element B, we translate B spatially. Then the neighborhood pixels are sorted to determine the infimum and supremum respectively. In next subsection, the method presented to sort the pixels is explained.

Through the combination of erosion and dilation operators, other operations can be defined. Firstly, we define the difference operator of color pixel value in RGB space.

Definition 16: Let f_1, f_2 be color images in RGB space. If $f_1(x) = (r_1(x), g_1(x), b_1(x))$, $f_2(x) = (r_2(x), g_2(x), b_2(x)), x \in \mathbb{R}^2$, the difference operator between f_1 and f_2 is defined as follows:

$$f_1(x) - f_2(x) = (|r_1(x) - r_2(x)|, |g_1(x) - g_2(x)|, |b_1(x) - b_2(x)|) \tag{14}$$

Definition 17: [32] Let f be a color image in RGB space and B be the structuring element, the following CMM operators are defined as:

- Opening

$$\gamma(f) = \delta(\epsilon(f)) \tag{15}$$

- Closing

$$\phi(f) = \epsilon(\delta(f)) \tag{16}$$

- Morphological gradient

$$\text{Grad}(f) = \delta(f) - \epsilon(f) \tag{17}$$

- Gradient by dilation

$$\text{Grad}_\delta(f) = \delta(f) - f \tag{18}$$

- Gradient by erosion

$$\text{Grad}_\epsilon(f) = f - \epsilon(f) \tag{19}$$

E. ORDER ON 3-GDFN SPACE

To define the morphological operators, it is necessary to sort the pixels of the structuring element to determine the minimum or maximum respectively. The core of color pixels sorting problem is to find the optimal pixel points according to certain criteria. This problem can be thought of as a multi-attribute decision problem with n alternatives (the number of pixels is n) and three attributes (three components of color image in the RGB space). The goal of the multi-attribute decision problem is to find the most acceptable alternative [42]. The goal here is to apply the decision strategy to select the appropriate pixels of the structuring element. The following definitions are proposed before introducing the total preorders in 3-GDFN space.

Let B be the structuring element, we define the ordering relation for the 3-GDFNs corresponding to the pixels in B.

Definition 18: Let $u, v \in$ 3-GDFN, $p = (p_1, p_2, p_3) \in \mathbb{R}^3$ with $p_1, p_2, p_3 \geq 0$ and $p_1 + p_2 + p_3 = 1$. Let $\overline{M}(u) = (\overline{x_1}, \overline{x_2}, \overline{x_3})$ and $\overline{M}(v) = (\overline{y_1}, \overline{y_2}, \overline{y_3})$ be the mean values of u, v, respectively. We define a binary relation in 3-GDFN space, that is a subset "$\prec^p$" of 3-GDFN $\times$ 3-GDFN as follows:

$$\prec^p = \{(u, v) \in \text{3-}GDFN \times \text{3-}GDFN : \sum_{i=1}^{3} p_i(\overline{y_i} - \overline{x_i}) \geq 0\} \tag{20}$$

If $(u, v) \in \prec^p$, then we say u to be smaller than v about $\prec^p$, and denote it as $u \prec^p v$.

Theorem 19: Let $p = (p_1, p_2, p_3) \in \mathbb{R}^3, p_1, p_2, p_3 \geq 0$ and $p_1 + p_2 + p_3 = 1$. Then

1) $u \prec^p u, \forall u \in$ 3-GDFN;
2) $u \prec^p v, v \prec^p w \Rightarrow u \prec^p w, \forall u, v, w \in$ 3-GDFN;

3) For any $u, v \in$ 3-GDFN, at least one of $u \prec^p v$ and $v \prec^p u$ is tenable.

Proof: Let $u, v, w \in$ 3-GDFN, $\overline{M}(u) = (\overline{x_1}, \overline{x_2}, \overline{x_3}))$, $\overline{M}(v) = (\overline{y_1}, \overline{y_2}, \overline{y_3}))$ and $\overline{M}(w) = (\overline{z_1}, \overline{z_2}, \overline{z_3})$.

1) $\overline{M}(u) \leq \overline{M}(u)$ for $\forall u \in$ 3-GDFN, then $u \prec^p u$.
2) Let $u \prec^p v$, $v \prec^p w$. Then we have $\sum_{i=1}^{3} p_i(\overline{y_i} - \overline{x_i}) \geq 0$ and $\sum_{i=1}^{3} p_i(\overline{z_i} - \overline{y_i}) \geq 0$. Hence, $\sum_{i=1}^{3} p_i(\overline{z_i} - \overline{x_i}) \geq 0$, i.e., $u \prec^p w$. So the transitivity of $\prec^p$ holds.
3) For any $u, v \in$ 3-GDFN, at least one of $\sum_{i=1}^{3} p_i(\overline{y_i} - \overline{x_i}) \geq 0$ and $\sum_{i=1}^{3} p_i(\overline{x_i} - \overline{y_i}) \geq 0$ is tenable. Then at least one of $u \prec^p v$ and $v \prec^p u$ is tenable.

□

By Theorem 19, we know that $\prec^p$ is fulfill the reflexivity, transitivity and completeness, so it is a total preorder on the 3-GDFN space. The following example shows that $\prec^p$ does not satisfy antisymmetry.

Example 20: Considering the pixels values provided in Example 11, the following matrixes are obtained:

$$[u]^0 = \begin{Bmatrix} (66, 128, 255) & (120, 24, 120) & (78, 88, 69) \\ (49, 137, 76) & (125, 100, 58) & (26, 25, 230) \\ (200, 46, 188) & (96, 58, 200) & (255, 203, 19) \end{Bmatrix}$$

$$[v]^0 = \begin{Bmatrix} (255, 66, 128) & (120, 120, 24) & (69, 78, 88) \\ (76, 49, 137) & (58, 125, 100) & (230, 26, 25) \\ (188, 200, 46) & (200, 96, 58) & (19, 255, 203) \end{Bmatrix}$$

According to (3), we can calculate that $\overline{M}(u) = (102, 78, 123)$ and $\overline{M}(v) = (123, 102, 78)$. When $p_1 = p_2 = p_3 = \frac{1}{3}$,

$$\sum_{i=1}^{3} p_i(\overline{y_i} - \overline{x_i}) = \frac{1}{3}((123 - 102) + (102 - 78) + (78 - 123)) = 0$$

$$\sum_{i=1}^{3} p_i(\overline{x_i} - \overline{y_i}) = \frac{1}{3}((102 - 123) + (78 - 102) + (123 - 78)) = 0$$

It means that $u \prec^p v$ and $v \prec^p u$ are both tenable. However, the u and v are different three generalized discrete fuzzy numbers.

Due to the $\prec^p$ is not antisymmetric, we will introduce another binary relation based on the 3-GDFN space. For $u, v \in$ 3-GDFN, $p = (p_1, p_2, p_3) \in \mathbb{R}^3$ with $p_1, p_2, p_3 \geq 0$ and $p_1 + p_2 + p_3 = 1$, $\overline{M}(u) = (\overline{x_1}, \overline{x_2}, \overline{x_3})$ and $\overline{M}(v) = (\overline{y_1}, \overline{y_2}, \overline{y_3})$ are the mean values of u, v, respectively. We denote $u \approx^p v$ if and only if $\sum_{i=1}^{3} p_i(\overline{y_i} - \overline{x_i}) = 0$. If $u \approx^p v$, we cannot differentiate u and v. Next, we introduce a new weak order relation based on the similarity definition 10. For this sake, we first give the Definition 21.

Definition 21: Let B be the structuring element, we represent the pixel value of each point in B as the 3-GDFN, denoted as $B' = \{u_i \in \text{3-GDFN} \mid i = 1, 2, \ldots, n, n \geq 2\}$. Then the similarity cumulative sum of $u_i \in B'$ is given by

$$\sigma_{sum}(u_i) = \sum_{j=1}^{n} \sigma(u_i, u_j) \tag{21}$$

where the $\sigma(u_i, u_j)$ is the similarity between two 3-GDFNs by (4).

Definition 22: Let $p = (p_1, p_2, p_3) \in \mathbb{R}^3$ with $p_1, p_2, p_3 \geq 0$ and $p_1 + p_2 + p_3 = 1$, and $B' = \{u_i \in \text{3-GDFN} : i = 1, 2, \ldots, n, n \geq 2\}$. We define a binary relation in 3-GDFN, that is a subset "$\lhd^p$" of 3-GDFN × 3-GDFN as follows:

$$\lhd^p = \prec^p_{\neq} \cup \lhd^p_{\approx} \tag{22}$$

where,

$\prec^p_{\neq} = \{(u, v) \in \text{3-GDFN} \times \text{3-GDFN} : u \prec^p v\} \setminus \{(u, v) \in \text{3-GDFN} \times \text{3-GDFN} : u \approx^p v\}$

$\lhd^p_{\approx} = \{(u, v) \in \text{3-GDFN} \times \text{3-GDFN} : u \approx^p v \text{ and } \sigma_{sum}(u) \leq \sigma_{sum}(v)\}$

If $(u, v) \in \lhd^p$, we say u to be smaller than v about $\lhd^p$, and denote it as $u \lhd^p v$.

Theorem 23: Let $p = (p_1, p_2, p_3) \in \mathbb{R}^3$ with $p_1, p_2, p_3 \geq 0$ and $p_1 + p_2 + p_3 = 1$, and $B' = \{u_i \in \text{3-GDFN} : i = 1, 2, \ldots, n, n \geq 2\}$. Then

1) The binary relation $\prec^p_{\neq}$ is transitive, but it is not reflexive and complete.
2) The binary relation $\lhd^p_{\approx}$ is transitive and reflexive, but it is not antisymmetric and complete.
3) The binary relation $\lhd^p$ is reflexivity, transitivity and completeness, but it is not antisymmetric. It is a total preorder on the 3-GDFN space.

Proof: We only prove the transitivity of $\lhd^p_{\approx}$, and the transitivity and the completeness of $\lhd^p$. The others are obvious. Let $u, v, w \in$ 3-GDFN, $\overline{M}(u) = (\overline{x_1}, \overline{x_2}, \overline{x_3}))$, $\overline{M}(v) = (\overline{y_1}, \overline{y_2}, \overline{y_3}))$ and $\overline{M}(w) = (\overline{z_1}, \overline{z_2}, \overline{z_3})$.

1) Let $u, v, w \in$ 3-GDFN, $u \lhd^p_{\approx} v$, $v \lhd^p_{\approx} w$. Then we have $\sum_{i=1}^{3} p_i(\overline{y_i} - \overline{x_i}) = 0$, $\sum_{i=1}^{3} p_i(\overline{z_i} - \overline{y_i}) = 0$, $\sigma_{sum}(u) \leq \sigma_{sum}(v)$, $\sigma_{sum}(v) \leq \sigma_{sum}(w)$. Hence, $\sum_{i=1}^{3} p_i(\overline{z_i} - \overline{x_i}) = 0$, $\sigma_{sum}(u) \leq \sigma_{sum}(w)$, i.e., $u \lhd^p_{\approx} w$. So the transitivity of $\lhd^p_{\approx}$ holds.
2) Let $u, v, w \in$ 3-GDFN, $u \lhd^p v$, $v \lhd^p w$. Then by the definition of $\lhd^p$, we have that $\sum_{i=1}^{3} p_i(\overline{y_i} - \overline{x_i}) > 0$ or $\sum_{i=1}^{3} p_i(\overline{y_i} - \overline{x_i}) = 0$, $\sigma_{sum}(u) \leq \sigma_{sum}(v)$, and $\sum_{i=1}^{3} p_i(\overline{z_i} - \overline{y_i}) > 0$ or $\sum_{i=1}^{3} p_i(\overline{z_i} - \overline{y_i}) = 0$, $\sigma_{sum}(v) \leq \sigma_{sum}(w)$. If $\sum_{i=1}^{3} p_i(\overline{y_i} - \overline{x_i}) > 0$ and $\sum_{i=1}^{3} p_i(\overline{z_i} - \overline{y_i}) > 0$, then $\sum_{i=1}^{3} p_i(\overline{z_i} - \overline{x_i}) > 0$, i.e., $u \lhd^p w$. If $\sum_{i=1}^{3} p_i(\overline{y_i} - \overline{x_i}) > 0$ and $\sum_{i=1}^{3} p_i(\overline{z_i} - \overline{y_i}) = 0$, $\sigma_{sum}(v) \leq \sigma_{sum}(w)$, then $\sum_{i=1}^{3} p_i(\overline{z_i} - \overline{x_i}) > 0$, i.e., $u \lhd^p w$. If $\sum_{i=1}^{3} p_i(\overline{y_i} - \overline{x_i}) = 0$, $\sigma_{sum}(u) \leq \sigma_{sum}(v)$ and $\sum_{i=1}^{3} p_i(\overline{z_i} - \overline{y_i}) > 0$, then $\sum_{i=1}^{3} p_i(\overline{z_i} - \overline{x_i}) > 0$, i.e., $u \lhd^p w$. If $\sum_{i=1}^{3} p_i(\overline{y_i} - \overline{x_i}) = 0$, $\sigma_{sum}(u) \leq \sigma_{sum}(v)$ and $\sum_{i=1}^{3} p_i(\overline{z_i} - \overline{y_i}) = 0$, $\sigma_{sum}(v) \leq \sigma_{sum}(w)$, then $\sum_{i=1}^{3} p_i(\overline{z_i} - \overline{x_i}) = 0$, $\sigma_{sum}(u) \leq \sigma_{sum}(w)$, i.e., $u \lhd^p w$. Thus,we have $u \lhd^p w$, the transitivity of $\lhd^p$ holds.
3) Let $u, v \in$ 3-GDFN. If $\sum_{i=1}^{3} p_i(\overline{y_i} - \overline{x_i}) \neq 0$, then $u \lhd^p v$ or $v \lhd^p u$ holds. If $\sum_{i=1}^{3} p_i(\overline{y_i} - \overline{x_i}) = 0$, then $\sigma_{sum}(u) \leq \sigma_{sum}(v)$ or $\sigma_{sum}(v) \leq \sigma_{sum}(u)$ holds, i.e., at least one of $u \lhd^p v$ and $v \lhd^p u$ is tenable. So the completeness of $\lhd^p$ holds.

□

Let B be the structuring element, we interpret the pixel value of each point in B as the 3-GDFN, denoted as $B' = \{u_i \in \text{3-GDFN} \mid i = 1, 2, \ldots, n, n \geq 2\}$. We define the infimum and supremum operations in B' by using the binary relation $\lhd^p$ as described earlier. Because $\lhd^p$ is a total preorder in 3-GDFN space, there is a situation that $u_i, u_j \in B'$, $i \neq j$ s.t. both $u_i \lhd^p u_j$ and $u_j \lhd^p u_i$ are tenable. In this case, we need to define the minimum and maximum between u_i and u_j firstly, so we denote $\min\{u_i, u_j\}$ and $\max\{u_i, u_j\}$, respectively.

Definition 24: Let $B' = \{u_i \in \text{3-GDFN} \mid i = 1, 2, \ldots, n, n \geq 2\}$, and $u_i, u_j \in B'$, $i \neq j$, the $\min\{u_i, u_j\}$ and $\max\{u_i, u_j\}$ are defined as follows:

$$\min\{u_i, u_j\} = \begin{cases} u_i, & \text{if } u_i \lhd^p u_j \\ u_j, & \text{if } u_j \lhd^p u_i \\ u_{\min\{i,j\}}, & \text{if both} \\ u_i \lhd^p u_j \text{ and } u_j \lhd^p u_i \text{ are tenable.} \end{cases} \tag{23}$$

$$\max\{u_i, u_j\} = \begin{cases} u_j, & \text{if } u_i \lhd^p u_j \\ u_i, & \text{if } u_j \lhd^p u_i \\ u_{\max\{i,j\}}, & \text{if both} \\ u_i \lhd^p u_j \text{ and } u_j \lhd^p u_i \text{ are tenable.} \end{cases} \tag{24}$$

Definition 25: Let $B' = \{u_i \in \text{3-GDFN} \mid i = 1, 2, \ldots, n, n \geq 2\}$, according to (23) and (24), the infimum and supremum operations in B' are defined as follows:

$$\inf B' = \min\{u_i | i = 1, 2, \ldots, n, n \geq 2\} \tag{25}$$

$$\sup B' = \max\{u_i | i = 1, 2, \ldots, n, n \geq 2\} \tag{26}$$

According to the definition of infimum and supremum operations on structuring element, the operators of color mathematical morphology can be constructed. Finally, the mean value of three-dimensional generalized discrete fuzzy numbers is calculated according to (3), and the three-dimensional generalized discrete fuzzy numbers processed by color mathematical morphology in 3-GDFNs space are mapped back to RGB space.

F. ANALYSIS

The basic operators properties, compatibility and computational complexity of the proposed CMM are analyzed in this subsection.

1) THE OPERATORS PROPERTIES ANALYSIS

Firstly, we analyze the properties of ϵ erosion operator and δ dilation operator defined in Definition 15 in the following. It is worth noting that when we investigate the properties of these operators, the shape of the structuring elements is fixed, which means that the value of λ defined in Section IV-C is 0.

Definition 26: The transformation ψ invariant to translations if it commutes with the translations.

Proposition 27: If ϵ and δ are erosion and dilation based on order $\leq_\tau$, then
ϵ is invariant to translations $\Leftrightarrow \epsilon(f \circ T_r) = \epsilon(f) \circ T_r$, $r \in \mathbb{R}^2$,
δ is invariant to translations $\Leftrightarrow \delta(f \circ T_r) = \delta(f) \circ T_r$, $r \in \mathbb{R}^2$.

Proof: Let $f : \mathbb{R}^2 \to \mathbb{R}^3$ be a color image, $y \in \mathbb{R}^2$,

$$\begin{aligned} \epsilon(f \circ T_r)(y) &= \inf_{x \in B}\{f \circ T_r \circ T_x(y)\} \\ &= \inf_{x \in B}\{f(y + x + r)\} \\ &= \inf_{x \in B}\{f(y + r + x)\} \\ &= \inf_{x \in B}\{f \circ T_x(y + r))\} \\ &= \epsilon(f)(y + r) \\ &= \epsilon(f) \circ T_r(y) \end{aligned}$$

Similarly, $\delta(f \circ T_r)(y) = \delta(f) \circ T_r(y)$. □

Definition 28: The transformation ψ is extensive if, for a color image f, the transformed image is greater than or equal to the original image. The transformation ψ is anti-extensive if, for a color image f, the transformed image is less than or equal to the original image.

Proposition 29: Let ϵ and δ are erosion and dilation based on order $\leq_\tau$, if the structuring element B contains the origin (i.e., $(0, 0) \in B$), then
ϵ is anti-extensive $\Leftrightarrow \epsilon(f) \leq_\tau f$,
δ is extensive $\Leftrightarrow f \leq_\tau \delta(f)$.

Proof: Let $f : \mathbb{R}^2 \to \mathbb{R}^3$ be a color image, according to the proposed definition of erosion operator,

$$\epsilon(f)(y) = \inf_{x \in B}\{f \circ T_x(y)\} = \inf_{x \in B}\{f(y + x)\},$$

$\forall y' \in \mathbb{R}^2$, $\exists \epsilon(f)(y') \leq_\tau f(y' + x)$, i.e., $\epsilon(f) \leq_\tau f$.
Similarly, $f \leq_\tau \delta(f)$. □

2) THE COMPATIBILITY ANALYSIS

The pixel value of gray-scale image or binary image is one-dimensional data, so it can be interpreted by one-dimensional generalized discrete fuzzy number. Correspondingly, the proposed ordering relationship in Section IV-E is compatible to the classical gray-scale (or binary) morphology when it is applied to gray-scale images (or binary). Therefore, the mathematical morphology for gray-scale images (or binary) can be obtained as a particular case of the proposed CMM.

Taking the color image in RGB space for example, the conversion between RGB and gray-scale is straightforward as shown in the following definition. Here, we assume that the value range of gray-scale image and each color component of RGB image is [0, 255].

Definition 30: The map π, that converts a color (r, g, b) in RGB space into a gray-scale value, is defined as:

$$\begin{aligned} \pi : RGB &\to [0, 255] \\ (r, g, b) &\mapsto r \end{aligned}$$

The map τ, that converts a gray-scale value a into a color value in RGB space, is defined as:

$$\begin{aligned} \tau : [0, 255] &\to RGB \\ a &\mapsto (a, a, a) \end{aligned}$$

That is, simply by reducing the color image in RGB space into the R channel provides a gray-scale version.

(a) (b) (c) (d) (e)

FIGURE 2. The original images in experiments. (a)Circle. (b)Tulips. (c)Peppers. (d)Lena. (e)Baboon.

The proposed operators constitute a generalization of the gray-scale morphological operators based on the threshold approach in [14].

Proposition 31: Let us consider the conversion between RGB colors and gray-scale value from the Definition 30. Then, the erosion and dilation operators proposed in Definition 15, when applied to gray-scale images, coincide with the corresponding operators from the threshold approach in [14] using the same structuring element.

Proof: We prove that, when restricted to gray-scale images, our operators provide the same results.

We consider the erosion operator firstly. Let g' be a gray-scale image, B be a structuring element. Then, the RGB conversion of g' is $\tau(g')$, where $\tau(g')(y) = (g'(y), g'(y), g'(y))$, $y \in \mathbb{R}^2$.

The erosion of $\tau(g')$ by B is then

$$\epsilon(\tau(g'))(y) = \inf_{x\in B}\{\tau(g') \circ T_x(y)\} = \inf_{x\in B}\{\tau(g')(y+x)\},$$

$\exists x_0 \in B$, s.t., the gray-scale projection of such image is:

$$\begin{aligned}\pi(\epsilon(\tau(g'))(y)) &= \pi(\inf_{x\in B}\{\tau(g')(y+x)\})\\ &= \pi(\tau(g')(y+x_0))\\ &= \pi(g'(y+x_0), g'(y+x_0), g'(y+x_0))\\ &= g'(y+x_0)\\ &= \inf_{x\in B}\{g'(y+x)\}\\ &= \inf_{x\in B}\{g' \circ T_x(y)\}\\ &= \epsilon(g')(y)\end{aligned}$$

Which matches the definition of erosion from the gray-scale morphological operator based on the threshold approach. The case for dilation is proved in a similar way. □

3) THE COMPUTATIONAL COMPLEXITY

And finally, the computational complexity of this approach associated to each step is also analyzed. Because the structuring element of this paper is variable according to the similarity of fuzzy numbers and the parameter λ, in order to calculate the computational cost of this method, the structuring element is specified as a rectangle containing n elements and $\lambda = 0$. First, the 3-GDFN representation of each pixel point in the structuring element is calculated, as shown in Section IV-B, this is an $O(n)$ step. Next, the fuzzy order relation is calculated. The complexity of the binary relation based on Definition 18 is $O(n)$. In the calculation of the binary relation based on Definition 22, the similarity of fuzzy numbers needs to be calculated, so this is an $O(n^2)$ step.

V. EXPERIMENTAL RESULTS AND ANALYSIS

In this section, many experiments are conducted to evaluate the effect of the proposed erosion operator, dilation operator and their combination. We discuss the results of experimentation, which were achieved using MATLAB R2018a, 64-bits installed in a PC with Intel(R) Core(TM)i5-8250U@1.60GHz CPU, 8.00 GB Dual-Channel DDR4 RAM, and Microsoft Windows 10 Home Edition (64-bits).

The original images used in these experiments are shown in Fig.2. These color images are $256 \times 256 \times 3$ pixels in the RGB space, and each channel of the images contains value between 0 and 255. The Fig.2a is a synthetic image made by Bouchet, et.al [32]. The Fig.2b, Fig.2c, Fig.2d and Fig.2e are selected from the CVG-UGR image database [43].

A. THE PROPOSED COLOR MATHEMATICAL MORPHOLOGY

First, the performance of the proposed method with 3-GDFN total preorder is studied. Fig.2a shows the original image used to check the effect of proposed operators. Because the Fig.2a is composed of points, circles, line segments, disks and other information, it has a clear foreground and background. The values of the experimental parameters are as follows, the structuring element is a square with a size of 5×5 pixels, and the value of parameter λ is 0, the parameters $p_1 = p_2 = p_3 = \frac{1}{3}$. The experimental results are shown in Fig.3.

Fig.3b and Fig.3c show that the dilation operator has an enlargement function that expands the objects brighter than the image background, while the erosion operator has a shrinkage function, so the small details in the image are removed, and the color and edges of larger objects become smoother. Both the opening and closing operators can suppress specific image details that are smaller than structuring elements, while ensuring that no global geometric distortion is generated. Fig.3d shows that the opening operation first removes the small bright details with erosion operator, then increases and restores the image brightness with dilation

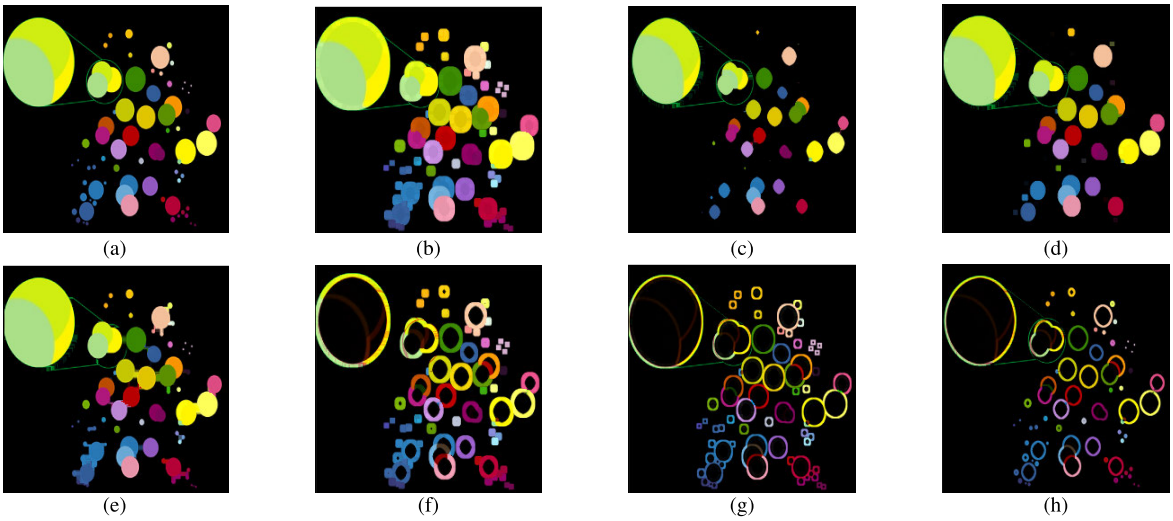

FIGURE 3. Effects of proposed operators with Figure 2a. (a)Original Image. (b)Dilation. (c)Erosion. (d)Opening. (e)Closing. (f)Morphological gradient. (g) Gradient by dilation. (h)Gradient by erosion.

operator, but does not re-introduce the previously removed details. The result of the closing operator is opposite to the opening operator. As shown in Fig.3e, the closing operator eliminates the small dark details while filling the small gaps between objects. The morphological gradient calculated by (17) is shown in Fig.3f. The boundary width calculated by the morphological gradient operator is two pixels. Because the dilation operator expands the bright area in the original color image by one pixel, and the erosion operator shrinks the bright area by one pixel. Correspondingly, Fig.3g and Fig.3h represent the single pixel edge in the image background and the single pixel edge belonging to the target, respectively.

The creation of new colors, also known as the false color problem, is sometimes described as a problem that needs to be overcome in mathematical morphology. However, in many applications of morphological processing, false colors are not completely unacceptable. For example, non-flat structuring elements can introduce false colors in gray-scale or color images, but can achieve better morphological filtering effects and smoother morphological gradients [25], [35]. As shown in Fig.3, there is false color phenomenon in the experimental results of dilation and erosion operators, which is caused by the independence of RGB spatial components interpreted by 3-GDFN. Moreover, the original image (Fig.2a) has distinct foreground and background, which makes the false color phenomenon more visually obvious. For morphological gradients, as shown in Equations (17), (18) and (19), because they are generated by vector subtraction, new colors will appear.

Next experiment is focused on comparing the different values of parameter λ in structuring elements. In order to explain the experimental effect more clearly, the original image as shown in Fig.2b and Fig.2c with rich texture are used.

We take a square matrix of 9×9 size as the initial structuring element in the original image Fig.2b, use the (4) to calculate the similarity between two pixels in this matrix, and set the parameter λ by the (10) to obtain the structuring element whose shape can change. Fig.4 shows the results of dilation and erosion operations about the flower image under different λ values. Comparing these experimental results, we can see that when the parameter value is 0.6, the dilation operator increases the overall brightness of the original image, while the erosion operator darkens the image as a whole and loses the image details (such as leaf veins and soil particles in Fig.4c). When the parameter value is 0.3, the result of the dilation operation in Fig.4d makes the white part of the petal edge significantly wider, while the result of erosion in Fig.4e causes the red part of the petal to be retained. When the parameter value is 0.1, the structuring element is closest to a square of 9×9 size, and the results of dilation and corrosion operations are Fig.4f and Fig.4g, respectively. We can see the more obvious block effect.

In addition, we take a 7×7 square in the original image Fig.2c as the initial structuring element, calculate the similarity using the same method and set the parameter λ. When the parameter value is 0.5, the results of the dilation operator and the erosion operator are shown in Fig.5b and Fig.5c, respectively. When the parameter value is 0.2, the results are shown in Fig.5d and Fig.5e. It can be seen from the (10) that the structuring elements are composed of pixels with fuzzy similarity greater than or equal to λ. Comparing the white boxes in Fig.5b and Fig.5d, we can see that the expansion effect is more obvious when the λ is larger, while in Fig.5c and Fig.5e, the contraction effects is more obvious when the λ is larger. The main reason is that the contrast of color pixels in the white box is relatively high, and the construction of the CMM operator in this paper fully considers the fuzzy similarity relationship between pixels.

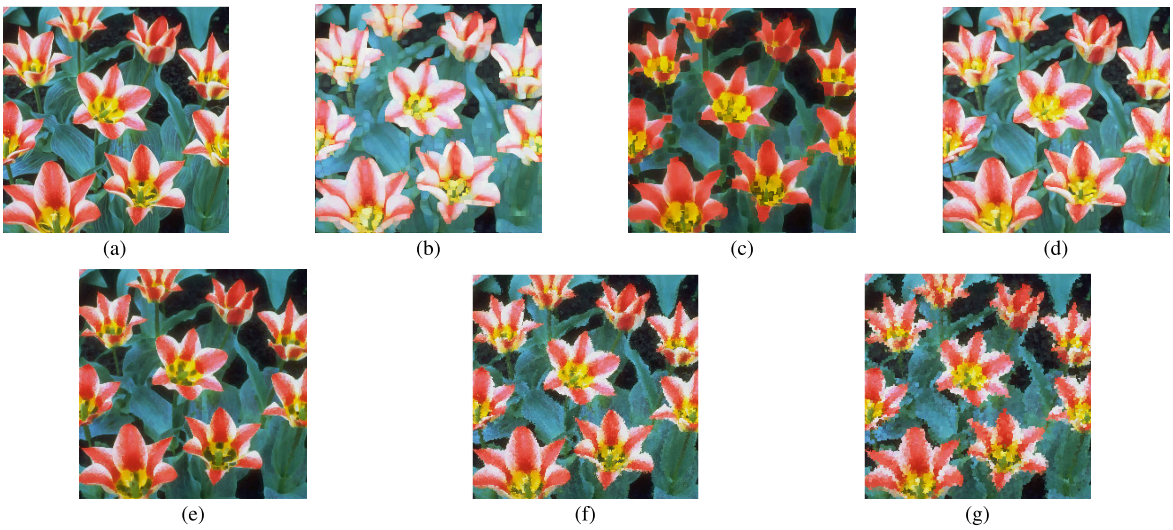

FIGURE 4. Effects of proposed operators with Figure 2b. (a)Original Image. (b)Dilation with $\lambda = 0.6$. (c)Erosion with $\lambda = 0.6$. (d)Dilation with $\lambda = 0.3$. (e)Erosion with $\lambda = 0.3$. (f)Dilation with $\lambda = 0.1$. (g)Erosion with $\lambda = 0.1$.

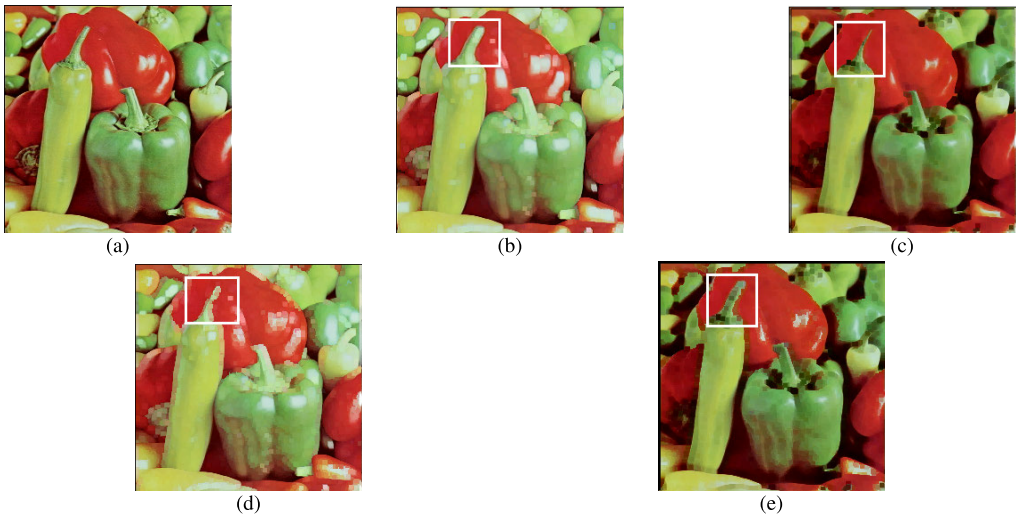

FIGURE 5. Effects of proposed operators with Figure 2c. (a)Original Image. (b)Dilation with $\lambda = 0.5$. (c)Erosion with $\lambda = 0.5$. (d)Dilation with $\lambda = 0.2$. (e)Erosion with $\lambda = 0.2$.

In this paper, on the basis of using 3-GDFN to represent pixels in the RGB color space, the basic CMM operators are defined according to the similarity of fuzzy numbers. In conclusion, we have considered not only the mean value feature of the pixels in structuring elements, but also the fuzzy similarity between the central pixel and its neighbors in this method. By setting different λ parameters, we can obtain structuring elements of different shapes, which can meet the requirements of different image processing applications.

B. COMPARISON WITH OTHER CMM

In this subsection, the key point of the experiments is to compare the proposed approach with other CMM methods in RGB space. The M-order is the Marginal ordering morphology method [25]. It is a straightforward extension of the gray-scale MM to color images. The lexicographic ordering approach [26] is the typical method in condition-ordering. We choose these two classical ordering methods to compare with the method in this paper. At the same time, since the erosion and dilation operators in [31] and [32] are both color morphology methods in RGB space, we also choose these two methods for comparison experiment.

We take Fig.2a and Fig.2e as the experimental object, and choose the square structuring elements with the size of 5×5 and 3×3 respectively. The order used by the lexicographic ordering method is first on red component then on green then on blue [26]. In [31], the authors order the color vectors in RGB space with respect to their distance to black pixel value (0,0,0) and white pixel value (255,255,255), we call this color morphological method extended from the threshold approach

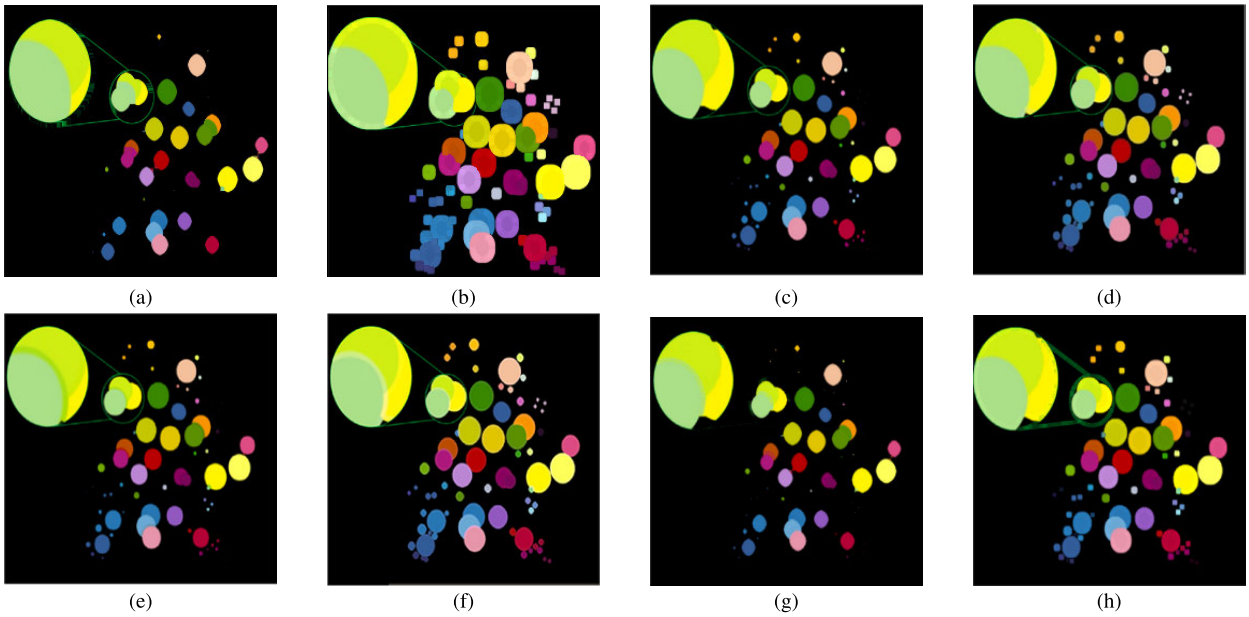

FIGURE 6. Comparison with fuzzy order [32], M-order, distance order [31] and proposed method. (a)Erosion with proposed method (Figure 3c). (b)Dilation with proposed method (Figure 3b). (c)Erosion with fuzzy order. (d)Dilation with fuzzy order. (e)Erosion with M-order. (f)Dilation with M-order. (g)Erosion with distance order. (h)Dilation with distance order.

as distance order morphological method. The fuzzy order in [32] is defined based on the fuzzy preference relation. The experimental results are shown in Fig.6 and Fig.7.

The experimental results in Fig.6 fulfill interpretability, that is, morphological operations make the bright objects in the original image (Fig. 2a) expand with dilation and shrink with erosion. Because the pixel points around the central pixel are taken into account when constructing 3-GDFN in this method, the shrinkage effect of erosion operator and expansion effect of dilation operator in this paper are more obvious under the condition of using the same structuring element. It can also be observed in Fig.6 that the proposed method avoids the notch on the edge of the largest disc caused by erosion and dilation operation.

As we have observed in Fig.7, there is a false color phenomenon in the proposed method and M-order method, for example, the part of the nose and its edge. However, the erosion and dilation defined by fuzzy order [32] and distance order [31] are color preserved. For the image with rich texture, the effect of fuzzy order [32] method is not better. When the proposed method is used, the structure and details of the image are preserved compared with other methods, such as the effect of the eye area.

Next, we compare the proposed method with other morphological methods in terms of running time. The operating environment for all methods is the same as the experimental environment mentioned at the beginning of Section V. The experimental object is Fig.2b and the structuring elements are the square with 3×3 size. The experimental results are shown in Fig.8. The horizontal axis represents all the morphological methods, while the vertical axis represents the running time and the unit of measurement is seconds. Among them, the running time of lexicographic order is the shortest, and the running time of M-order and distance order methods is slightly longer than that of lexicographic order. The fuzzy order method runs longer than them because the fuzzy preference relation of vectors has to be calculated. The proposed method needs to construct the 3-GDFN representation of color vectors before vector sorting, so the running time is the longest. As shown in Fig.8, when λ takes on different values, the algorithm operates at different speeds because of the different number of objects in the structuring element which need to be sorted.

Since there is no obvious quantitative standard, it is difficult to quantitatively compare mathematical morphology methods with the results given by basic operators [41]. In next subsection, we use the noise reduction and texture classification in color images to prove the objective advantages of the method proposed in this paper.

C. COLOR NOISE REDUCTION

Next, the performance of the proposed CMM operators is tested about color noise reduction quality. In order to compare with other morphological algorithms, we add the uncorrelated zero-mean Gaussian noise (variance $\sigma = 32$ and $\rho = 0$) to the original images (Fig.2b, Fig.2c, Fig.2d and Fig.2e). In the real world, noise is often not caused by a single source, but by many different sources. Assuming that the actual noise is regarded as the sum of many random variables with different probability distributions, and each random variable is independent, the central limit theorem shows that as the number of noise sources increases, their normalize sums approach the Gaussian distribution. Based on this assumption, the

FIGURE 7. Comparison with fuzzy order [32], M-order, distance order [31] and proposed method. (a)Original Image (Figure 2e). (b)Erosion with proposed method. (c)Dilation with proposed method. (d)Erosion with fuzzy order. (e)Dilation with fuzzy order. (f)Erosion with M-order. (g)Dilation with M-order. (h)Erosion with distance order. (i)Dilation with distance order.

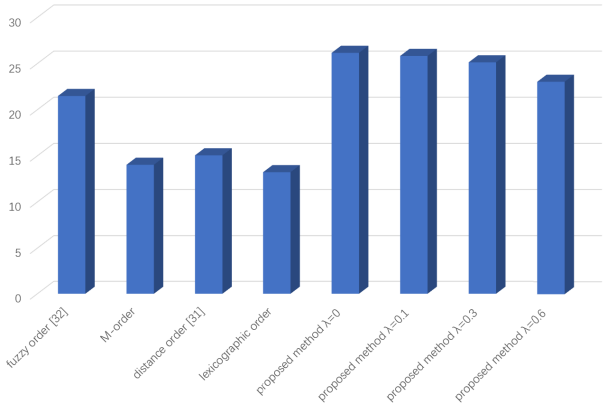

FIGURE 8. Comparison with other methods in terms of running time. The unit of time is seconds.

Gaussian noise is a simple approximate simulation for the complex and unknown noise distribution.

We use the open-close close-open(OCCO) filter algorithm to achieve smooth filtering of noisy images. A square structuring element with a size of 3×3 pixels is used in the noisy image, and the OCCO filter is defined as follows:

$$OCCO(f(i,j)) = \frac{1}{2}\phi(\gamma(f(i,j))) + \frac{1}{2}\gamma(\phi(f(i,j))) \quad (27)$$

where ϕ and γ denote the opening and closeing operators in (15) and (16), respectively.

Correspondingly, the normalized mean squared error (NMSE) is used to measure the quality of denoised image.

$$NMSE = \frac{\sum_{i=1}^{M}\sum_{j=1}^{M}\|f(i,j) - f'(i,j)\|^2}{\sum_{i=1}^{M}\sum_{j=1}^{M}\|f(i,j)\|^2} \quad (28)$$

TABLE 1. NMSE × 100 values of images after noise reduction by the OCCO filter algorithm.

	proposed order	M-order	Lexicographic order
Tulips	0.92	0.98	2.63
Peppers	0.98	1.09	3.31
Lena	0.82	0.78	2.29
Baboon	1.18	1.27	2.53

TABLE 2. NMSE × 100 values of images after noise reduction by the traditional median filter algorithm.

	Median with proposed order	Median with M-order	Median with Lexicographic order
Tulips	1.39	1.76	3.98
Peppers	1.43	1.56	4.36
Lena	1.22	1.35	3.68
Baboon	1.69	1.86	4.06

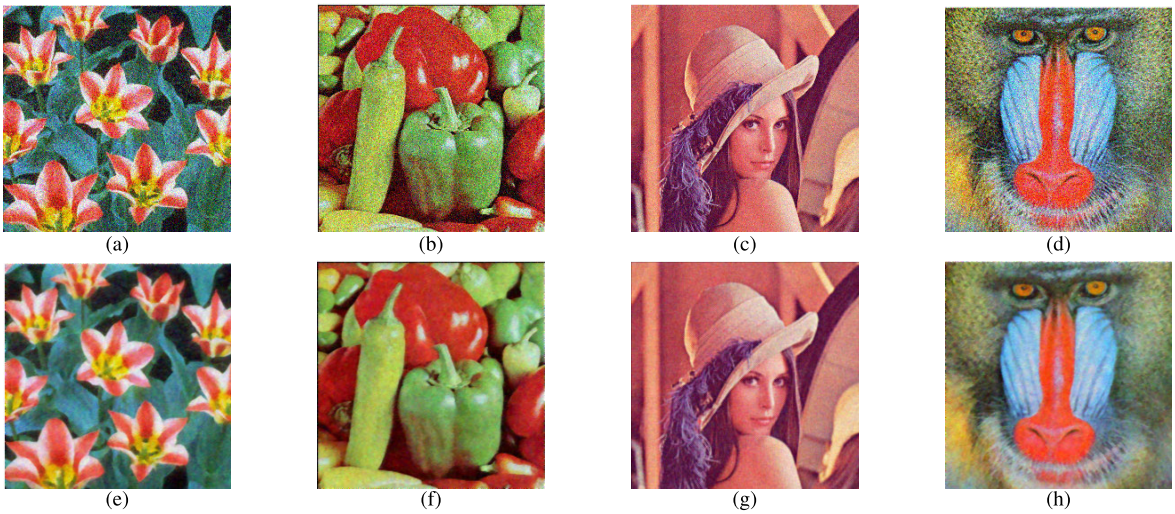

FIGURE 9. Images corrupted with uncorrelated zero-mean Gaussian noise (variance $\sigma = 32$ and $\rho = 0$) and color noise reduction by OCCO filter algorithm. (a)The Tulips image adding noise. (b)The Peppers image adding noise. (c)The Lena image adding noise. (d)The Baboon image adding noise. (e)The denoised Tulips image. (f)The denoised Peppers image. (g)The denoised Lena image. (h)The denoised Baboon image.

where $f(i, j)$ and $f'(i, j)$ denote the vectorial pixels at position (i, j) for the original and filtered images respectively, while $\|\cdot\|$ represents the Euclidean norm.

The image after removing the noise using the OCCO algorithm defined by the operators in this paper is shown in Fig.9. In addition, we selected the M-order morphological method and lexicographic order morphological method for comparative experiment. The square structuring element of 3×3 pixels is also selected and applied to the OCCO smoothing filter in Fig.9a, Fig.9b, Fig.9c and Fig.9d respectively. The M-order (Marginal ordering) corresponds to univariate ordering implemented at each component of a given vectors. Data is arranged independently along each of its channels. The order used by the lexicographic ordering method is first on red component then on green then on blue.

Table 1 shows the NMSE results of the method for removing uncorrelated zero-mean Gaussian noise. According to the obtained values, the superiority of the proposed method and M-order approach are remarkable, and lexicographic order method has the worst denoising effect. Although the NMSE value of proposed method is close to M-order, as mentioned earlier, the M-ordering is the pointwise ordering method of the color components, which will produce a more obvious false colors in original image. Since the correlation between color components is not considered in the lexicographic order method, the NMSE value is the largest.

We also compare the OCCO filtering algorithm with the traditional median filtering method and take the Fig.9a, Fig.9b, Fig.9c and Fig.9d as examples. We consider the proposed order, M-order and Lexicographic order to sort the color pixel and select the median value. Similarly, the template size of the median filter is the same as the structuring element size in the OCCO filter method. The experimental results are shown in Table 2. By comparing the results in Table 1 and Table 2, it can be seen that the noise reduction effect of the OCCO filtering algorithm is better than that of the traditional median filtering method.

D. COLOR TEXTURE CLASSIFICATION

In order to further verify the performance of the CMM operator proposed in this paper, we use the texture classification algorithm presented in [25] on the Outex-13 texture database [44] to verify the accuracy rates of texture classification of different morphological operators. There are 68 types of texture images in the Outex-13 database. Each type contains 10 texture images for the training set and the test set. The same category of texture image is acquired from the same object during multiple times. There are a specific angle of view and rotation angle in each image. According to literature [45], we use normalized morphological covariance as the color texture descriptor.

$$k(f) = \frac{Vol(\epsilon_{p_{2,v}}(f))}{Vol(f)} \tag{29}$$

TABLE 3. Classification rates in percent for textures of Outex13, using erosion based covariance.

	proposed order	fuzzy order	M-order	Lexicographic order
RGB	78.02	77.20	77.65	70.74

where the normalized morphological covariance k of image f, Vol is the volume of f (i.e. sum of pixel values), eroded by a pair of points $\epsilon_{p_{2,\nu}}$ separated by a vector ν.

We selected the M-order, lexicographic order and fuzzy order [32] for comparative experiment. All results were obtained using the k-nearest neighbors (K-NN) algorithm and Euclidean distance on the Outex-13 database. Table 3 shows the accuracy rates of texture classification by (29) for the morphological erosion operators, which were constructed with different vector ordering methods. The CMM method proposed in this paper has a texture classification accuracy rate significantly greater than the lexicographic orders method.

Fuzzy order method is defined based on fuzzy preference relation, it allows giving the same importance to all the components of the image. However, we further considered the distribution of surrounding pixels when constructing 3-GDFN, so the corresponding texture classification accuracy rate was higher.

VI. CONCLUSION

In this paper, based on the study of the generalized discrete fuzzy numbers basic theory, the 3-GDFN has been applied to the mathematical morphology processing of color images. By calculating the fuzzy similarity of 3-GDFNs, the total preorder relations of 3-GDFN space has been defined, and the color dilation and color erosion operators based on structuring elements have been constructed. Experimental results have shown that these operators can be used for color image morphology processing and achieved better results in color image noise reduction and texture classification. The color mathematical morphology method in this paper is an extension of the traditional gray-scale method. The advantage of the algorithm is that it can process color image and is compatible with the traditional gray-scale method. The future work is mainly to combine fuzzy set theory to consider non-flat structuring elements and design new color morphological operators.

REFERENCES

[1] S. S. L. Chang and L. A. Zadeh, "On fuzzy mapping and control," *IEEE Trans. Syst., Man, Cybern.*, vol. SMC-2, no. 1, pp. 30–34, Jan. 1972.
[2] W. Voxman, "Canonical representations of discrete fuzzy numbers," *Fuzzy Sets Syst.*, vol. 118, no. 3, pp. 457–466, Mar. 2001.
[3] G. Wang, C. Wu, and C. Zhao, "Representation and operations of discrete fuzzy numbers," *Southeast Asian Bull. Math.*, vol. 29, no. 5, pp. 1003–1010, 2005.
[4] J. Casasnovas and J. V. Riera, "Extension of discrete t-norms and t-conorms to discrete fuzzy numbers," *Fuzzy Sets Syst.*, vol. 167, no. 1, pp. 65–81, Mar. 2011.
[5] J. V. Riera and J. Torrens, "Aggregation of subjective evaluations based on discrete fuzzy numbers," *Fuzzy Sets Syst.*, vol. 191, pp. 21–40, Mar. 2012.
[6] J. V. Riera and J. Torrens, "Aggregation functions on the set of discrete fuzzy numbers defined from a pair of discrete aggregations," *Fuzzy Sets Syst.*, vol. 241, pp. 76–93, Apr. 2014.
[7] S. Massanet, J. V. Riera, J. Torrens, and E. Herrera-Viedma, "A new linguistic computational model based on discrete fuzzy numbers for computing with words," *Inf. Sci.*, vol. 258, pp. 277–290, Feb. 2014.
[8] J. V. Riera, S. Massanet, E. Herrera-Viedma, and J. Torrens, "Some interesting properties of the fuzzy linguistic model based on discrete fuzzy numbers to manage hesitant fuzzy linguistic information," *Appl. Soft Comput.*, vol. 36, pp. 383–391, Nov. 2015.
[9] J. V. Riera and J. Torrens, "Using discrete fuzzy numbers in the aggregation of incomplete qualitative information," *Fuzzy Sets Syst.*, vol. 264, pp. 121–137, Apr. 2015.
[10] G. Wang and J. Wang, "Generalized discrete fuzzy number and application in risk evaluation," *Int. J. Fuzzy Syst.*, vol. 17, no. 4, pp. 531–543, Dec. 2015.
[11] G. Wang, P. Shi, Y. Xie, and Y. Shi, "Two-dimensional discrete fuzzy numbers and applications," *Inf. Sci.*, vol. 326, pp. 258–269, Jan. 2016.
[12] M. Zhao, M.-Y. Liu, J. Su, and T. Liu, "A shape similarity-based ranking method of hesitant fuzzy linguistic preference relations using discrete fuzzy number for group decision making," *Soft Comput.*, vol. 23, no. 24, pp. 13569–13589, Dec. 2019.
[13] B. D. Ripley and G. Matheron, "Random sets and integral geometry," *J. Roy. Stat. Soc.*, vol. 139, no. 2, pp. 277–278, 1976.
[14] J. Serra, *Image Analysis and Mathematical Morphology*, vol. 1. London, U.K.: Academic, 1982.
[15] M. Jourlin, B. Laget, G. Matheron, F. Meyer, F. Preteux, M. Schmitt, and J. Serra, *Image Analysis and Mathematical Morphology*, vol. 2. London, U.K.: Academic, 1988.
[16] S. R. Sternberg, "Grayscale morphology," *Comput. Vis. Graph. Image Process.*, vol. 35, pp. 333–355, Sep. 1986.
[17] B. D. Baets, *A Fuzzy Morphology: A Logical Approach*. New York, NY, USA: Springer, 1998.
[18] I. Bloch and H. Maitre, "Fuzzy mathematical morphologies: A comparative study," *Pattern Recognit.*, vol. 28, no. 9, pp. 1341–1387, Sep. 1995.
[19] M. Nachtegael and E. E. Kerre, "Classical and fuzzy approaches towards mathematical morphology," in *Fuzzy Techniques in Image Processing*, vol. 52. 2000, pp. 3–57.
[20] M. Nachtegael and E. E. Kerre, "Connections between binary, gray-scale and fuzzy mathematical morphologies," *Fuzzy Sets Syst.*, vol. 124, no. 1, pp. 73–85, Nov. 2001.
[21] T. Mélange, M. Nachtegael, P. Sussner, and E. E. Kerre, "On the construction of interval-valued fuzzy morphological operators," *Fuzzy Sets Syst.*, vol. 178, no. 1, pp. 84–101, Sep. 2011.
[22] P. Sussner, M. Nachtegael, T. Mélange, G. Deschrijver, E. Esmi, and E. Kerre, "Interval-valued and intuitionistic fuzzy mathematical morphologies as special cases of $\mathbb{L}$-fuzzy mathematical morphology," *J. Math. Imag. Vis.*, vol. 43, no. 1, pp. 50–71, May 2012.
[23] E. Aptoula and S. Lefèvre, "A comparative study on multivariate mathematical morphology," *Pattern Recognit.*, vol. 40, no. 11, pp. 2914–2929, Nov. 2007.
[24] V. Barnett, "The ordering of multivariate data," *J. Roy. Statal Soc. A, General*, vol. 139, no. 3, pp. 318–344, 1976.
[25] J. J. van de Gronde and J. B. T. M. Roerdink, "Group-invariant colour morphology based on frames," *IEEE Trans. Image Process.*, vol. 23, no. 3, pp. 1276–1288, Mar. 2014.
[26] E. Aptoula and S. Lefèvre, "On lexicographical ordering in multivariate mathematical morphology," *Pattern Recognit. Lett.*, vol. 29, no. 2, pp. 109–118, Jan. 2008.
[27] S. Velasco-Forero and J. Angulo, "Random projection depth for multivariate mathematical morphology," *IEEE J. Sel. Topics Signal Process.*, vol. 6, no. 7, pp. 753–763, Nov. 2012.
[28] O. Lezoray, "Complete lattice learning for multivariate mathematical morphology," *J. Vis. Commun. Image Represent.*, vol. 35, pp. 220–235, Feb. 2016.
[29] M. C. d'Ornellas and J. A. T. B. D. Costa, "Color mathematical morphology based on partial ordering of spectra," in *Proc. 20th Brazilian Symp. Comput. Graph. Image Process. (SIBGRAPI)*, Oct. 2007, pp. 37–44.
[30] M. A. Veganzones, M. D. Mura, G. Tochon, and J. Chanussot, "Binary Partition Trees-based spectral-spatial permutation ordering," in *Proc. Int. Symp. Math. Morphol. Appl. Signal Image Process.*, 2015, pp. 434–445.
[31] V. D. Witte, S. Schulte, M. Nachtegael, D. V. D. Weken, and E. E. Kerre, "Vector morphological operators for colour images," in *Proc. 2nd Int. Conf. Image Anal. Recognit. (ICIAR)*, Toronto, ON, Canada, Sep. 2005, pp. 667–675.

[32] A. Bouchet, P. Alonso, J. I. Pastore, S. Montes, and I. Díaz, "Fuzzy mathematical morphology for color images defined by fuzzy preference relations," *Pattern Recognit.*, vol. 60, pp. 720–733, Dec. 2016.
[33] T. Lei, Y. Zhang, Y. Wang, S. Liu, and Z. Guo, "A conditionally invariant mathematical morphological framework for color images," *Inf. Sci.*, vol. 387, pp. 34–52, May 2017.
[34] M. E. Valle and R. A. Valente, "Mathematical morphology on the spherical CIELab quantale with an application in color image boundary detection," *J. Math. Imag. Vis.*, vol. 57, pp. 183–201, Feb. 2017.
[35] P. Bibiloni, M. González-Hidalgo, and S. Massanet, "Soft color morphology: A fuzzy approach for multivariate images," *J. Math. Imag. Vis.*, vol. 61, pp. 394–410, Mar. 2019.
[36] A. Bouchet, S. Montes, V. Ballarin, and I. Díaz, "Intuitionistic fuzzy set and fuzzy mathematical morphology applied to color leukocytes segmentation," *Signal, Image Video Process.*, vol. 14, no. 3, pp. 557–564, Apr. 2020.
[37] H. M. Al-Otum, "A novel set of image morphological operators using a modified vector distance measure with color pixel classification," *J. Vis. Commun. Image Represent.*, vol. 30, pp. 46–63, Jul. 2015.
[38] Y. Li, K. Qin, and X. He, "Some new approaches to constructing similarity measures," *Fuzzy Sets Syst.*, vol. 234, pp. 46–60, Jan. 2014.
[39] D.-G. Wang, Y.-P. Meng, and H.-X. Li, "A fuzzy similarity inference method for fuzzy reasoning," *Comput. Math. Appl.*, vol. 56, no. 10, pp. 2445–2454, Nov. 2008.
[40] J. Angulo, "Morphological colour operators in totally ordered lattices based on distances: Application to image filtering, enhancement and analysis," *Comput. Vis. Image Understand.*, vol. 107, nos. 1–2, pp. 56–73, Jul. 2007.
[41] A. Căliman, M. Ivanovici, and N. Richard, "Probabilistic pseudo-morphology for grayscale and color images," *Pattern Recognit.*, vol. 47, no. 2, pp. 721–735, Feb. 2014.
[42] L. Wang and N. Li, "Pythagorean fuzzy interaction power bonferroni mean aggregation operators in multiple attribute decision making," *Int. J. Intell. Syst.*, vol. 35, no. 1, pp. 150–183, Jan. 2020.
[43] C. U. of Granada. *CVG-UGR Image Database*. Accessed: 2014. [Online]. Available: http://decsai.ugr.es/cvg/dbimagenes/c512.php
[44] T. Ojala, T. Maenpaa, M. Pietikainen, J. Viertola, J. Kyllonen, and S. Huovinen, "Outex-new framework for empirical evaluation of texture analysis algorithms," in *Proc. 16th Int. Conf. Pattern Recognit.*, vol. 1, Aug. 2002, pp. 701–706.
[45] E. Aptoula and S. Lefèvre, "Spatial morphological covariance applied to texture classification," in *Multimedia Content Representation, Classification and Security* (Lecture Notes in Computer Science), vol. 4105, no. 1. 2006, pp. 522–529.

ZENGTAI GONG was born in Gansu, China, in 1965. He received the Ph.D. degree from the Harbin Institute of Technology, China. He is currently a Professor and a Ph.D. Supervisor with the College of Mathematics and statistics, Northwest Normal University, China. His research interests include real analysis theory, rough set, fuzzy analysis, and applications in environment problems and management of water resources. He is a member of the Editorial Board of Fuzzy Sets and Systems.

NA QIN was born in Gansu, China, in 1982. She received the B.S. degree in computer science and technology and the master's degree in computer application technology from Northwest Normal University, China, in 2004 and 2007, respectively, where she is currently pursuing the Ph.D. degree. Her main research interests include fuzzy inference systems, fuzzy sets, rough sets and their applications.

GUICANG ZHANG was born in Gansu, China, in 1964. He received the Ph.D. degree from the Northwestern Polytechnical University, China. He is currently a Professor with the College of Mathematics and Statistics, Northwest Normal University, China. His research interests include image process, digital watermarking, and computer aided geometric design.